HHS Public Access

Author manuscript

Pharm Res. Author manuscript; available in PMC 2021 November 02.

Published in final edited form as:

Pharm Res. ; 37(12): 235. doi:10.1007/s11095-020-02959-w.

Simultaneous pharmacokinetic analysis of nitrate and its reduced metabolite, nitrite, following ingestion of inorganic nitrate in a mixed patient population

Andrew R. Coggan[1], **Susan B. Racette**[2], **Dakkota Thies**[2], **Linda R. Peterson**[2], **Robert E. Stratford Jr.**[3,*]

[1]Department of Kinesiology[1], Indiana University Purdue University, Indianapolis, IN 46202

[2]Department of Medicine, Washington University School of Medicine, St. Louis, MO 63110

[3]Division of Clinical Pharmacology, Department of Medicine, Indiana University School of Medicine, Indianapolis, IN 46202

Abstract

Purpose: The pharmacokinetic properties of plasma NO_3^- and its reduced metabolite, NO_2^-, have been separately described, but there has been no reported attempt to simultaneously model their pharmacokinetics following NO_3^- ingestion. This report describes development of such a model from retrospective analyses of concentrations largely obtained from primary endpoint efficacy trials.

Methods: Linear and non-linear mixed effects analyses were used to statistically define concentration dependency on time, dose, as well as patient and study variables, and to integrate NO_3^- and NO_2^- concentrations from studies conducted at different times, locations, patient

*Corresponding Author Robert E. Stratford Jr., Indiana University School of Medicine, Research II, 950 West Walnut Street, Indianapolis, IN 46202, robstrat@iu.edu.

7.4. Author contributions

All authors contributed to the study conception and design. Material preparation, data collection and analysis were performed by Andrew R. Coggan and Robert E. Stratford, Jr. The first draft of the manuscript was written by Robert E. Stratford, Jr. and all authors commented on previous versions of the manuscript. All authors read and approved the final manuscript.

6. Data Availability

The datasets generated during and/or analyzed during the current study are available from the corresponding author on reasonable request.

7. Disclosures

7.1. Competing Interests

The authors have no financial or non-financial interests to disclose.

7.3. Ethics approval and informed consent

Approval for studies conducted in St. Louis was obtained from the Human Research Protection Office at Washington University in St. Louis. Approval for studies in Indianapolis was obtained from the Human Subjects Office at Indiana University. Written informed consent was obtained from each subject.

groups, and several studies in which sample range was limited to a few hours. Published pharmacokinetic studies for both substances were used to supplement model development.

Results: A population pharmacokinetic model relating NO_3^- and NO_2^- concentrations was developed. The model incorporated endogenous levels of the two entities, and determined these were not influenced by exogenous NO_3^- delivery. Covariate analysis revealed intersubject variability in NO_3^- exposure was partially described by body weight differences influencing volume of distribution. The model was applied to visualize exposure versus response (muscle contraction performance) in individual patients.

Conclusions: Extension of the present first-generation model, to ultimately optimize NO_3^- dose versus pharmacological effects, is warranted.

Keywords

nitric oxide; nitrate; nitrite; pharmacokinetics; isokinetic dynamometry

1. Introduction

Decline in skeletal muscle function, such as occurs as a consequence of natural aging (1), or due to heart failure (2–4), is a significant contributor to reduced quality and length of life (5). With expected doubling by 2050 in the number of persons 65 years or older, strategies for addressing this decline are needed. Clearly, routine exercise plays a role in delaying decline in muscle function and in preserving muscle mass (6). At the tissue and cellular levels, research designed to understand the physiological underpinnings of muscle function decline with aging or with heart failure has identified nitric oxide (NO) as a key player (7–13).

In single muscle fibers and isolated muscles, NO increases the speed of maximal muscle contraction and maximal generated power (7). Age and disease-associated decline of NO concentrations are associated with declines in these measures of muscle function (14–16). This decrease in NO is the result of both reduced formation and increased loss. With respect to formation, decreased expression of the neuronal form of NO synthase, which is the major isoform of this enzyme responsible for formation of NO in muscle from L-arginine and O_2, is partially responsible for decreased NO in muscle (16–18). Increased loss of NO in muscle is attributed to increased oxidative stress (14, 15). A primary consequence of reduced NO in muscle is a decline in flow-mediated vasodilation (19–22), which is directly correlated with muscular power and physical functioning (23). The more recent understanding that NO can be generated by successive reduction of NO_3^- and NO_2^- (24–26) evidences the critical role NO plays in regulating muscle function and movement.

Studies in rodents (27–30) and more recently humans (31, 32), have shown that muscle is a reservoir for NO_3^-, and that low oxygen tension and low pH generated during exercise, facilitate reductase-mediated conversion to NO to support contraction, as well as stimulate blood flow through NO-mediated vasodilation. Elucidation of this alternate pathway for NO

generation has led to several studies to evaluate the effects of dietary NO_3^- and ingestion of NO_3^--rich foods, such as beetroot juice (BRJ), on skeletal muscle function and blood pressure (33–37). Overall positive findings have stimulated research designed to address the role that various dietary sources and NO_3^- formulations have on exposure to NO_3^- and NO_2^-. James, et al (38) provide an excellent review of these studies. One study determined that the absolute bioavailability of NO_3^- from several dietary sources was 100% (39). The absolute oral bioavailability of NO_2^- following $NaNO_2$ administration was also determined to be approximately 100%, and was rapidly absorbed, with peak times ranging from 15 to 45 minutes (40). Another study conducted in Type 2 diabetics following oral administration of an immediate release formulation of $NaNO_2$ also observed peak times in the same range (41).

Several studies have been conducted to describe the pharmacokinetic properties related to distribution and elimination of NO_3^- or NO_2^- following administration of NO_3^- or NO_2^-,respectively. The half-life of NO_2^- following intravenous administration of 0.12 mmol of $NaNO_2$ was approximately 30 min (40). Decline in concentration was mono-phasic, thus indicating rapid distribution and elimination. Descriptive pharmacokinetic analysis (C_{max}, t_{max}, AUC and half-life) of NO_3^- have been described following intravenous administration and NO_3^- ingestion to healthy volunteers (39, 42–45). Like NO_2^-, mono-phasic decline also supports a conclusion of rapid distribution of NO_3^-. Half-life of NO_3^- from either route was 5 to 10 hours. Average clearance and volume of distribution were 2.9 L/h and 21 L in two separate studies (39, 42), one following oral ingestion and the other following intravenous infusion. In two studies in which time courses of both NO_3^- and NO_2^- were determined out to 24 hours after NO_3^- ingestion, C_{max} for NO_3^- was approximately 2–3 hours, while NO_2^- C_{max} was later (approximately 3.5 hours). The delay for NO_2^- is attributed to the time it takes for plasma NO_3^- to be concentrated in saliva, reduced to NO_2^- by oral bacteria and subsequently absorbed in the intestine (46–48).

Given the clinical importance of the NO_3^-/NO_2^-/NO reduction pathway for its positive benefits on skeletal muscle function and the cardiovascular system (49, 50), understanding the relational pharmacokinetics of these substances following oral NO_3^- ingestion is important. Conceivably, elucidating the potential role of several variables (e.g., diet, age, heart function, sex, and liver and renal function) on absorption and reductive metabolism could be important to optimizing the therapeutic effects of this source of NO.

The purpose of the reported study was to contribute to the goal of NO_3^- dose optimization by developing a first-generation model to describe the pharmacokinetics of NO_3^- and its reduced metabolite, NO_2^- following NO_3^- ingestion. Application of a non-linear mixed effects population analysis was essential to model development. Of note, the majority of the concentration data used to support model development were limited to < 3 hours following

administration. Those data came from studies designed to evaluate the effects of NO_3^- ingestion on muscle function rather than from studies designed to evaluate pharmacokinetic properties. Thus, in order to inform the model, data from published pharmacokinetic studies for NO_3^- and NO_2^- were also used.

2. Materials and Methods

2.1. Subjects

Pharmacokinetic model development was supported by measurement of NO_3^- and NO_2^- plasma concentrations in 42 subjects evaluated in the clinical laboratories of the co-authors, either affiliated with Washington University in St. Louis, or Indiana School of Medicine, Indianapolis. Concentrations from four clinical studies registered in ClinicalTrials.gov were used: NCT01682356 and NCT02797184 conducted in St. Louis, and NCT03513302 and NCT03595774 conducted in Indianapolis. Measurement of muscle contractile function was the chief aim of these studies, and was evaluated in 37 of the 42 subjects. Subjects were recruited to support investigation of the effects of oral NO_3^- on muscle contractile function in either healthy elderly subjects, or in patients with HFrEF. Six of the 14 elderly subjects were studied in St. Louis, and the remaining eight were studied in Indianapolis. These subjects were nondiabetic and considered in good health, as assessed by physical examination and standard blood chemistries. With respect to enrollment of elderly subjects, exclusion criteria included age below 65 or above 79 years, or history of significant cardiovascular (e.g., Stage II or greater hypertension, heart failure, and myocardial inflation/ischemia), renal (estimated glomerular filtration rate < 60 mL/min/1.73 m^2, or 61–90 mL/min/1.73 m^2, and albumin-creatinine ratio > 300, or liver disease (serum glutamic-oxaloacetic transaminase/serum glutamic pyruvic transaminase > 2x normal), anemia (hematocrit < 30%), or any other contraindication to strenuous exercise. Those taking phosphodiesterase inhibitors (e.g., sildenafil) were excluded, as these can potentiate nitric oxide effects (51).

For the 28 patients with a diagnosis of HFrEF, studies were conducted in St. Louis. The diagnosis of HFrEF was based on systolic dysfunction, i.e., an ejection fraction (EF) of <45%, as based on an echocardiogram obtained within the last 12 mo. Subjects had to be ≥18 y of age, on a stable HF treatment regimen (i.e., no addition, removal, or change in medication dose of >100% in the last 3 mo), and without significant orthopedic limitations or other contraindications to exercise. Subjects were excluded if they had major organ system dysfunction other than HF or were pregnant or were unable to give informed consent.

For both groups, additional exclusion criteria included use of antacids or proton pump or xanthine oxidase inhibitors, which can influence reduction of NO_3^- and NO_2^- to NO (52). Individuals taking phosphodiesterase inhibitors (e.g., Viagra) were also excluded, as these can potentiate NO effects (53).

2.2. Experimental Design and Protocol

A double-blind, placebo-controlled randomized crossover design was applied for all 14 elderly subjects, and in 17 of the 28 patients with HFrEF. In the elderly subject group, six subjects received either placebo, or an 11.2 mmol dose of NO_3^-. An additional seven subjects received placebo, a dose ranging from 11.8 to 16.8 mmol of NO_3^- (15 mmol/70 kg), and a higher dose of NO_3^- ranging from 23.5 to 33.7 mmol (30 mmol/70 kg) on three separate occasions using a three-way randomized crossover design. One elderly subject received placebo followed by a 23.7 mmol NO_3^- dose. Seventeen of 23 of the HFrEF patients were administered in randomized crossover fashion either placebo or an 11.2 mmol dose of NO_3^-. In all crossover studies, washout period between doses was one or two weeks. Six patients in the HFrEF group received a 10 mmol NO_3^- dose and a 20 mmol NO_3^- dose administered in a randomized crossover fashion with a one-week period between doses. The remaining five of the HFrEF patients received a 10 mmol dose of NO_3^- on a single occasion.

2.1.1. NO_3^- **formulations—**Elderly subjects consumed beetroot juice (BRJ) formulated to contain a measured concentration of NO_3^- as certified by the supplier (Beet It Sport, James White Drinks, Ipswich, UK) and confirmed via direct measurement. Patients diagnosed with heart failure either received BRJ or were administered capsules containing potassium nitrate (KNO_3). For subjects receiving BRJ, placebo was prepared by the supplier by removing NO_3^- using an ion exchange resin, but with preservation of taste, smell and texture as previously reported (54). In subjects administered NO_3^- from KNO_3 capsules, placebo capsules contained cornstarch powder.

2.2.2. NO_3^- **administration—**In crossover studies pertaining to either healthy elderly subjects or patients with HFrEF, subjects reported to the clinical research site in the morning after avoiding high NO_3^- foods (e.g., arugula, beets, spinach) for the previous 24 hours and any food, caffeine, and alcohol for the previous 12 hours. During this period, they also refrained from chewing gum, brushing their teeth, or using an antibacterial mouthwash, as these can block reduction of NO_3^- to NO_2^- by oral bacteria (55). Following measurement of seated heart rate and blood pressure, an intravenous catheter was placed in an antecubital vein and 6 mL of blood was drawn, anticoagulated with EDTA, and immediately centrifuged for 10 min at 3500 g at 4° C. Plasma was removed and frozen at −80° C for subsequent measurement of plasma NO_3^- and NO_2^- concentrations using high performance liquid chromatography (HPLC), as detailed below in section 2.2.3.

In all cases, NO_3^- administration was in the fasted state. Following NO_3^- administration, subjects rested quietly, with additional measurements of heart rate, blood pressure, and plasma NO_3^- and NO_2^- obtained 1 and 2 hours after NO_3^- ingestion. Muscle contractile function was then measured during the third hour post- NO_3^- ingestion (described in section 2.2.4.), with final measurements of hemodynamics and NO_3^-/NO_2^- concentrations obtained

approximately 10 minutes post-exercise. Subjects were then released from the clinical unit. After a 1–2 weeks washout period, subjects returned for up to two additional visits during which they were "crossed over" to receive a different dose of NO_3^-, or placebo, with the above described procedures repeated.

In five of the 28 patients with HFrEFF, blood samples were collected pre-dose, and at 1, 2, 3, 4.5, 6, 12, 18, and 24 hours following BRJ administration containing 10 mmol of NO_3^-. Muscle contractile function was not assessed in these five patients.

2.2.3. Quantitative analysis of NO_3^- and NO_2^-—Plasma NO_3^- and NO_2^- concentrations were measured using a dedicated HPLC analyzer (ENO-30, Eicom USA, San Diego, CA). In this system, NO_3^- and NO_2^- are isolated from each other and from interfering substances on a polystyrene gel separation column, NO_3^- reduced to NO_2^- on a cadmium column, and both reacted with Griess reagent followed by spectrophotometric detection at 540 nm. Retention times for NO_2^- and NO_3^- are ~4 and ~8 min, respectively. For analysis, 25 μL of thawed plasma was deproteinized 1:1 with methanol, centrifuged for 10 min at 10000 g at 4° C, and 10 μL of the protein-poor supernatant manually injected into the HPLC. Peak areas on the chromatograms were integrated using the manufacturer's EPC-700 Envision software. The assay limit of quantitation was 0.07 μM and 0.007 μM for NO_3^- and NO_2^-, respectively. This method was highly reproducible, with test-retest correlation coefficients of 0.99 and 0.98 for NO_3^- and NO_2^-, respectively. To further reduce variability, all samples from a single subject were analyzed at the same time.

2.2.4. Measurement of muscle contractile function—The procedure used for measurement of contractile properties of the quadriceps muscle group has been described in detail in our previous studies (54, 56, 57). Briefly, measurements are made using an isokinetic dynamometer (Biodex System 4 Pro, Biodex Medical Systems, Shirley, NY). Following alignment of the lateral femoral epicondyle of the subject's dominant leg with the axis of rotation of the dynamometer, they performed maximal knee extensions at angular velocities of (in order) 0, 1.57, 3.14, 4.71, and 6.28 rad/s (0, 90, 180, 270, and 360°/s). Subjects executed 3–4 maximal efforts at each velocity and were allowed two minutes of rest after each set of contractions. Isometric testing was conducted at a knee joint angle of 1.22 rad (70°). Peak torque was expressed relative to body mass (ie, in N·m/kg), after which peak power (in W/kg) at each velocity was calculated by multiplying peak torque by velocity. Maximal knee extensor power (P_{max}, in W/kg) and angular velocity (ω_{max}, in rad/s) were then analyzed by fitting an inverted parabola to the peak power-velocity relationship as detailed in a previous publication (54).

2.3. Statistical Analysis

A linear-mixed effects (LME) approach was used to evaluate the effects of independent variables (time, dose, age, body weight, heart function, sequence, period) on observed NO_3^- and NO_2^- concentrations at baseline, and 1 and 2 hours following oral NO_3^- administration

to the 42 subjects evaluated in four separate placebo-controlled randomized crossover studies. The total number of samples analyzed was 276 and 275 for plasma NO_3^- and NO_2^-, respectively. LME statistical analysis informed pharmacokinetic model development, which incorporated endogenous NO_3^- and NO_2^- concentrations to support a model structure in which these concentrations were stable across time. Given the complex source of the data used to build the integrated NO_3^- and NO_2^- pharmacokinetic model (crossover design from mixed populations over four studies), LME was considered a necessary first step. Phoenix WinNonlin 8.1 (Certara L.P., Princeton, NJ) was used. The level of statistical significance to support an effect was $p<0.05$. Given the crossover design used, each subject served as his or her own control in the assessment of concentration variance.

2.4. Pharmacokinetic Modeling

To further support model development, particularly with respect to the elimination phase, mean plasma NO_3^- and NO_2^- data were obtained from published studies. These are summarized in Supplementary Table 1. For NO_3^-, these data were obtained from three studies (42, 43, 58), all administering NO_3^- in the fasted state (consistent with our studies). In one study (42), mean plasma NO_3^- was reported in numerical format out to 48 hours. In the other two studies, Engauge Digitizer (https://github.com/markummitchell/engauge-digitizer/releases) was used to convert graphical mean plasma NO_3^- and NO_2^- concentrations to numerical form. To further support NO_2^- pharmacokinetics, digitized data were obtained from a reported study in which NaNO2 was administered by IV infusion, or orally (40). Two studies measured both plasma NO_3^- and NO_2^- following NO_3^- administration (as KNO_3 or beetroot juice) to healthy males and females (44, 45); however, these data were not added to support model development since either body weight (to support its influence as a covariate on concentrations), or NO_3^- dose were not reported.

Population modeling was based on non-linear mixed effects (NLME) analysis using Phoenix NLME 8.1 (Certara L.C., Princeton, NJ). NLME simultaneously estimates population-level parameters (fixed effects), and random effects attributable to unexplained interindividual variability (IIV) in parameters and left-over residual unexplained variability (RUV) in concentrations. Concentrations of NO_3^- and NO_2^- as a function of time were expressed as ordinary differential equations (summarized in the Appendix).

First Order Conditional Estimation (FOCE) and Quasi-Random Parametric Expectation Maximization (QRPEM) estimation methods were evaluated to support the NLME approach. FOCE was ultimately used based on its consistent reliability to provide estimates of parameter precision in the combined NO_3^-/NO_2^- model. Model building was sequential, beginning with plasma NO_3^-, followed by inclusion of plasma NO_2^-. For both model building stages, incorporation of between-subject variability random effects on model parameters without covariance was evaluated for each structural parameter, except for clearance and volume of distribution, or baseline concentrations. In these cases, covariance

terms on these random effects were also estimated. Random effects were modeled as $parameter_{indiv} = parameter_{pop} * exp(eta_{indiv})$, where eta is the difference of an individual's specific parameter estimate relative to the population estimate; thus, a log-normal distribution of parameters across the subject population was assumed. Residual unexplained variability (RUV) in concentrations was modeled as a fixed error, or a proportional error, or a combined fixed plus proportional error. A proportional error model provided the best description of this variability, where, for a specific concentration, observed concentration = predicted concentration * (1 + error). Attempts were made to reduce unexplained inter-subject random variability by evaluating the effect of incorporating known differences between subjects as covariates. Incorporation of several potential covariates was attempted at each stage. Covariates examined were age, weight (normalized to 70 kg), heart function, and sex. Influence of these variables was evaluated for baseline concentration, clearance, volume of distribution, and NO_2^- formation clearance. Age and body weight were treated as continuous covariates; whereas, heart function and sex were treated as categorical covariates (0 for normal heart function and 1 for patients with diagnosed HFrEF). Significant covariates were identified by testing all possible combinations of covariates and looking for reduction in −2LL (−2 times the log of the likelihood objective function output from model fitting). Covariate models with reductions in −2LL relative to the base model (no covariates) were then nested in the base model and a likelihood ratio test conducted. This metric follows a Chi-square distribution, with a reduction in −2LL > 3.84 being statistically significant at the $p < 0.05$ level. Significant covariates in the NO_3^- alone model were carried forward to the combined NO_3^-/NO_2^-.

Goodness of model fit at each of the two model development phases was based on precision of the fixed effect parameter estimates, and graphical analyses of observed concentrations versus the model predicted concentrations at the population and individual subject levels, the latter after taking account between subject random effects and covariates. Balance of the data across the line of identity over the entire concentration range was considered ideal. In addition, conditional weighted residuals (CWRES) over the population predicted concentration range and over time were evaluated to determine the percentage of CWRES within the −2 to 2 limits. Individual observed versus predicted concentration-time profiles were also inspected. A visual predictive check of the final combined NO_3^-/NO_2^- model was used to evaluate the ability of the model to predict the variability in observed concentrations. This consisted of simulation of 1,000 hypothetical subjects based on the final model parameters and their precision. A bootstrap analysis from 200 fits to the final model structure, based on random selection with replacement of the 42 subjects, was conducted to verify stability and precision of the various model parameter estimates. The final model was also used to simulate concentrations following a once-daily dose regimen of 24.3 mmol of NO_3^-, and compared to measured NO_3^- and NO_2^- concentrations in two elderly subjects receiving this regimen for 13 days (14 doses). Thirty simulations were conducted for each of the original 42 subjects. Mean concentrations were calculated for each subject, and summarized across this population as median predicted concentrations with their NO_3^- and NO_2^- associated 90% confidence intervals.

3. Results

3.1. Subject demographics

The population pharmacokinetic model describing the relationships between NO_3^- and NO_2^- concentrations was developed from two groups of subjects: patients with HFrEF and healthy elderly subjects. Table I provides a summary of their physical characteristics according to these two classifications.

3.2. Statistical analyses of concentrations

3.2.1. Baseline concentrations—

Concentrations of NO_3^- and NO_2^- in plasma were determined prior to administration in all subjects receiving a dose of NO_3^-. In addition, concentrations were determined at 1 and 2 hours following placebo administration. Mean ± standard error of the mean (SEM) NO_3^- concentrations were 35.7 ± 1.66 μM (154 observations), while NO_2^- concentrations were 0.31 ± 0.022 μM (153 observations). Relative standard deviation (coefficient of variation) was 58% and 90% for NO_3^- and NO_2^-, respectively. Concentrations of NO_2^- were 8.6% of NO_3^- concentrations. Baseline NO_3^- and NO_2^- plasma concentrations were similar to those reported in our previous studies and by others (38, 43, 59–61).

Linear mixed effects analysis of NO_3^- and NO_2^- concentrations following administration of placebo indicated the NO_3^- concentrations were not different between pre-placebo administration and 1- and 2-hours following placebo administration. The same was true for NO_2^- concentrations. There was no influence of period, sequence (order of administration), or heart function on placebo NO_3^- and NO_2^- concentrations. Specific to heart function, observed lack of a difference between healthy elderly and patients with HFrEF agrees with reported absence of a difference between age- and sex-matched healthy versus HFrEF patients with respect to combined NO_3^- and NO_2^- plasma concentrations (62). Conclusions were the same when baseline concentrations were incorporated (concentrations measured prior to administration of a NO_3^- dose).

3.2.2. Concentrations at 1 and 2 hours—

Concentrations of NO_3^- and NO_2^- measured at 1- and 2-hours were significantly higher ($p<0.05$) following NO_3^- administration relative to placebo. Average concentrations pre-dose and at these two time points are summarized in Figure 1. For NO_3^-, there was a significant increase in these concentrations when NO_3^- dose was increased from an average dose of 11.6 mmol (ranging from 10.0 to 16.8 mmol) to 24.3 mmol (ranging from 20.0 to 33.7 mmol); however, NO_2^- concentrations were not different between these two dose levels. Body weight influenced NO_3^- concentrations, but not NO_2^- concentrations. Specifically, as body weight increased, NO_3^- concentrations decreased. While heart function had no effect on baseline

concentrations, there was a statistically significant lowering of NO_3^- concentrations (but not NO_2^- concentrations) in patients with HFrEF compared to healthy elderly subjects ($p=0.047$) when evaluating pre-dose, 1- and 2-hour concentrations. There was no effect of period or sequence on NO_3^- and NO_2^- concentrations.

3.3. Pharmacokinetics

The two stages of model development, NO_3^- model alone, followed by the combined NO_3^- and NO_2^- model, incorporated endogenous (i.e., baseline) NO_3^- and NO_2^- concentrations. As supported by linear mixed effects analysis of concentrations following placebo administration, or prior to NO_3^- administration, these concentrations were treated as time invariant following NO_3^- administration. As such, they reflect the redox interconversion equilibrium between reduction of NO_3^- and oxidation of NO_2^- (63). NO_3^- alone and NO_3^- and NO_2^- models based on net concentrations following exogenous NO_3^- administration, that is, concentrations after subtracting average baseline concentrations, resulted in similar model parameter estimates. This analysis confirmed that biochemical processes influencing endogenous levels of the two molecular entities were not altered following NO_3^- ingestion.

The final model structure unifying the kinetics of NO_3^- and NO_2^- is shown in Figure 2. Although oxidation of metabolite NO_2^- back to NO_3^- following NO_3^- ingestion should be possible, a model structure including an interconversion clearance term could not be developed. Lack of identifiability in this parameter was attributed to the much larger NO_3^- concentrations arising from ingestion relative to interconversion. Pharmacokinetic parameter estimates were stable when all dose levels, including placebo, were modeled simultaneously. This indicated that the pharmacokinetic parameters of the two molecular entities were constant over the ingested NO_3^- dose range, with predicted concentrations of each increasing in proportion to dose. Observed concentrations of plasma NO_3^- and NO_2^- were modeled according to a 1-compartment model structure. NO_3^- absorption following ingestion was modeled as a first order process. This structure was supported based on measured concentrations out to 24 hours in five patients with HFrEF (Figure 3). In these patients, NO_3^- concentrations peaked between 1 and 3 hours; terminal half-life ranged from 7 to 26 hours (Mean = 14 hours). While time to peak concentration was similar to observations by others following doses between 3 and 5 mmol to healthy adults (42, 43, 61), estimated half-life appeared generally longer than the half-life estimates reported in these studies (5 and 7.5 hours on average, respectively). As also apparent in Figure 3, decline in metabolite NO_2^- concentrations was parallel to decline in NO_3^- concentrations, consistent with the fact that this reduced metabolite has faster elimination kinetics than NO_3^-, such that its elimination following NO_3^- administration is rate-determined by its formation from NO_3^-. In support of this, an approximate 0.5 hour NO_2^- half-life following its intravenous

and oral administration has been reported (40). The time to maximum NO_2^- concentrations ranged from 3 to 6 hours following NO_3^- ingestion.

Pharmacokinetic parameter estimates for NO_3^- were stable for the two models. Supplementary Table 2 summarizes parameter estimates for the isolated NO_3^- model. Table II provides a summary of estimates for the final model incorporating the two molecular entities. In general, these parameters were well estimated (%RSD < 20%). Model goodness-of-fit plots for the final model combining the two molecular entities are summarized in Supplementary Figures 1 – 5. It was not possible to estimate between-subject variability on all parameters. This was most likely due to insufficient determinations over a sufficient time (24 hours or longer) in most subjects. Inter-subject variability of baseline concentrations was estimated and found to be most variable for NO_2^- (> 100%).

Based on dose normalized ratios of NO_2^- to NO_3^- exposures (AUCs) following oral NO_3^- ingestion, and the population clearance estimates of the two entities (CL), the fraction of absorbed NO_3^- metabolized to NO_2^- (f_m) was 3.0% ($AUC_{NO2-}/AUC_{NO3-} = f_m * (CL_{NO3-}/CL_{NO2-})$. In the two models, the only statistically significant covariate was the influence of body weight on the volume of distribution of NO_{3-}, which increased with body weight according to the relationship $V = V_{pop} *$ normalized weight$^{\wedge covariate}$, where V_{pop} is the population estimate. This result is consistent with aforementioned statistical analysis demonstrating decreased NO_3^- concentrations as body weight increased (Section 3.2.2.). Increasing volume of distribution with body weight is a common occurrence for low molecular weight (< 500) substances (64). Although statistical analysis also identified that NO_3^- concentrations were higher in patients with HFrEF compared to healthy elderly subjects (Section 3.2.2.), including a categorical covariate of heart function on NO_3^- clearance did not result in a statistically significant improvement of model fit ($p = 0.061$). Quite possibly, with a larger population of subjects in these two categories, decreased cardiac output and hence renal blood flow would be found to result in reduced ability to eliminate NO_3^-. Population-level estimates of NO_3^- clearance and volume of distribution were similar to those reported previously (42, 43, 65).

A visual predictive check simulating NO_3^- and NO_2^- concentrations in 1,000 simulated subjects indicated reliable performance of the final model (Supplementary Figure 6). Median predicted concentrations were similar to median observed concentrations for both molecular forms. In a bootstrap analysis based on random sampling with replacement to generate 200 different subject populations, each also consisting of 42 subjects, the range of estimates for the various parameters are also summarized in Table II. These were consistent with those obtained in the combined NO_3^- and NO_2^- model. The final model was used to predict concentrations in two elderly subjects following a daily NO_3^- dose of 24.3 mmol for 13 days. Results demonstrated good prediction of concentrations after 7 and 13 doses (Supplementary Figure 7).

The final model was used to simulate exposures to NO_3^- and NO_2^- over 24 hours following a dose of NO_3^-, expressed as $AUC_{0–24h}$. In a previously reported study in elderly subjects there was an overall increase in these two measures following NO_3^- ingestion (56). A significant increase ($p < 0.05$) in these two measures was also observed in the present study as exposure to NO_3^- and NO_2^- increased from baseline levels after a dose of NO_3^-. Figure 4 shows the relationship between $AUC_{0–24h}$ for NO_3^-, and change in either maximal angular velocity of knee extension or maximal power of knee extension in subjects in which these measures of muscle contractile function were made. As also observed in the cited study, the response was differential, that is, muscle function increased in most subjects, but was unaffected in some.

4. Discussion

A pharmacokinetic model describing the effect of NO_3^- ingestion on plasma levels of NO_3^- and its reduced metabolite, plasma NO_2^-, has been developed. The basic structure modeled NO_3^- absorption as a first order process with a half-life of approximately 40 minutes ($\ln(2)/1.1\ h^{-1}$)× 60 min/h). Between subject variability for the first order rate constant for NO_3^- absorption was 77.4% (Table II). The influence of NO_3^- formulation on NO_3^- and NO_2^- plasma kinetics has been extensively evaluated and summarized (38). A recent study evaluated the effects on kinetics from several NO_3^- formulations derived from beets (61). Altogether, these studies indicated that both time to peak concentration and extent of absorption can be influenced by formulation and/or by co-administration with food. The present analysis, conducted in fasted subjects, did not detect a difference in rate of absorption of NO_3^- in KNO_3 versus NO_3^- from beetroot juice. This may have been due to imbalance with respect to this potential determinant, as only 11 of the 42 subjects received KNO_3. These 11 subjects were from one clinical trial designed to evaluate KNO_3 palatability to support its use (for relative consistency of supply) in future Phase 2 and 3 clinical trials. Most likely due to insufficient measurement of NO_3^- and NO_2^- concentrations beyond 2 hours post-administration, we were not able to measure between subject variability on CL, which is influenced by extent of absorption; thus, we could not determine if the two formulations were different in this respect. To date, there are no systematic evaluations (e.g. crossover studies) demonstrating different absorption characteristics of these two sources of exogenous NO_3^-. A cross-sectional study by Kapil, et al (45) in healthy volunteers reported similar dose-normalized plasma NO_3^- and NO_2^- concentrations following ingestion of KNO_3 versus beetroot juice.

The time to maximum NO_2^- concentration was delayed by approximately 1.0 to 1.5 hours in the five patients with HFrEF for which concentration time courses were determined out to 24 hours. Simulated peak NO_2^- concentrations in all 42 subjects were also delayed by approximately 1 hour. Others have found similar results, both with respect to the time to

peak for NO_3^- and NO_2^-, as well as a difference in peak time of about an hour (59, 61). The delay in NO_2^- relative to NO_3^- peak concentrations is expected, and indicates good model performance in describing the reductive metabolic process.

Development of a model that linked NO_3^- and NO_2^- concentrations was facilitated by a study that measured NO_2^- exposure following both intravenous and oral NO_2^- administration (40). Knowledge of the pharmacokinetics following intravenous dosing provided estimates of distribution (V) and elimination (CL) of NO_2^- unbiased by absorption processes. Consequently, the model was able to estimate the fraction of NO_3^- elimination due to formation of NO_2^-. Based on population estimates summarized in Table II, the ratio of predicted NO_2^- formation clearance (Cl_f) to predicted total NO_3^- clearance (f_m) was 2.5% ($f_m = Cl_f/Cl_{NO3-}$), and compares well with the estimate of 3.0% (Table II and Results section 3.3.) based on dose-normalized AUC ratios of NO_2^- to NO_3^-.

In addition to evaluating heart function and body weight as sources of inter-subject variability in exposure to NO_3^- and NO_2^-, possible influences of age and sex were also evaluated. Given the small number of subjects representing racial groups other than White, there was no attempt to look at race as a covariate. The potential effects of kidney and liver function were also not evaluated, as measures of function of these organs were not consistently taken during the studies. Although summed NO_3^- and NO_2^- plasma concentrations have been shown to decline with age (15), an age effect was not evident in the present analysis. Most likely, inability to demonstrate an age-related effect on these concentrations is due to a smaller range of ages and more subjects focused to ages between 65 – 80 years. With respect to sex, there was no effect in the present analysis. A study involving healthy premenopausal women observed that baseline NO_3^- concentrations were not different in males and females; however, baseline NO_2^-, and summed NO_3^- and NO_2^- concentrations following a KNO_3 oral dose of 24 mmol were higher in females (45). However, these differences could be due to lower body mass in females (which, in fact, was reported to be statistically significantly lower in the study), and associated reduced volume of distribution and clearance, both of which would result in higher plasma concentrations. Additional and sufficiently powered studies in elderly subjects and HFrEF patients would need to be conducted to determine the possible effect of sex in these two groups.

A differential knee extension velocity and power response to ingested NO_3^- (Figure 4) is similar to that reported previously by our group (57). That study related these muscle performance measures to NO_3^- dose (placebo versus a 13.4 mmol dose delivered in beetroot juice) in elderly subjects. The present analysis related these same muscle function measures, butto model-derived simulated plasma NO_3^- exposure (rather than dose) in subjects encompassing a larger range of ages and with normal versus diseased heart function. The results in Figure 4 express this relationship to NO_3^- $AUC_{0–24h}$. The same patterns were

observed with respect to AUC for NO_2^-, and exposure based on C_{max} for both molecular entities (data not shown). Consistency among these various measures of exposure in relation to observed muscle function over doses ranging from placebo (baseline-endogenous exposure) to approximately 25 mmol NO_3^- indicates consistent within subject NO_3^- absorption and reduction over a broad dose range. This being said, there was substantial interindividual variability in these exposure measures. Possible causes are variability in NO_3^- absorption, variability in metabolic processes, including the reduction step, and variability in elimination of both molecular entities. Hypothesis-driven studies in additional subjects and associated modeling efforts would be able to quantify, rank and mechanistically describe these various sources, which is a prerequisite to understanding and describing the exposure versus response pharmacodynamic relationship.

While the pharmacokinetic parameters for NO_3^- and NO_2^- were constant over a range of exposures, it is not possible in this data set to determine the relationship between plasma exposure to NO_3^- and NO_2^-, and muscle function. Clearly across the 42 subjects there was variability in muscle function, with performance increasing over the exposure range in most, but with some evidence of saturation, and even a decline in some subjects. The pharmacodynamics of NO_3^-/NO_2^-/NO causative of alterations in muscle function are poorly characterized. Experiments eliciting a range of exposures with temporal measures of muscle function in individuals would be useful. Incorporating other biomarkers of muscle anatomy and physiology, such as fast- versus slow-twitch fiber analysis, would also be helpful to better understand and thereby predict these exposure – function relationships.

A limitation in the present analysis was that concentration measures beyond 2 hours postadministration were limited; however, this is the advantage of the population modeling approach, which is to develop model-based descriptions of pharmacokinetic and pharmacodynamic data in a sample-constrained environment common in clinical trials. Notably, the model did a good job predicting concentrations observed in a multiple dose regimen.

5. Conclusions

A single dose pharmacokinetic model that simultaneously describes NO_3^- and NO_2^- concentrations in plasma has been developed. The model connects the two molecular entities through reductive metabolism of the ingested and absorbed NO_3^-. The derived model can be used to design future studies to confirm its structure (time and dose independent kinetics, and dependence of NO_3^- concentrations on body weight), and expand understanding of other important determinants of exposure (e.g. age, sex, hepatic and renal function, heart function) and effect on muscle performance, and how the latter may vary over prolonged daily dosing.

Supplementary Material

Refer to Web version on PubMed Central for supplementary material.

Acknowledgments

7.2. Funding

This study was supported by grant HL121661 from the National Heart, Lung, and Blood Institute (NHLBI), grant AG053606 from the National Institute on Aging (NIA), grant AR072581 from the National Institute on Arthritis and Musculoskeletal and Skin Disease (NIAMS), and grants UL1 TR000448 and UL1 TR002529 from the National Center for Advancing Translational Sciences (NCATS) of the National Institutes of Health (NIH). Its contents are solely the responsibility of the authors and do not necessarily represent the official views of the NHLBI, NIA, NIAMS, NCATS, or NIH.

9.: Appendix – Model Equations for Final Model

dA1na/dt = − (CLna * Cna) + (Aana * Kana)); A1na = 0 at time = 0

dA1ni/dt = − (CLni * Cni) + (CLfni * Cna) + (Aani * Kani)); A1ni =0 at time = 0 (oral NO_3^- dosing); A1ni = dose at time = 0 (intravenous NO_2^- dosing)

dAana/dt = − (Aana * Kana)); Aana = NO_3^- oral dose = 0 at time = 0

dAani/dt = − (Aani * Kani)); Aani = NO_3^- oral dose = 0 at time = 0

Cna = A1na / Vna

Cni = A1ni / Vni

Definitions:

A1 = amount in central compartment (μmol); Aa = amount in absorption compartment (μmol). Cna = NO_3^- concentration in plasma (μM); Cni = NO_2^- concentration in plasma (μM). dA/dt is the rate of change in the amount (μmol) in the central compartment per unit time. All other abbreviations are as defined in Table II.

Abbreviations:

AUC	Area-under-the-curve
BRJ	beetroot juice
CL	clearance
F	absolute bioavailability
HFrEF	heart failure reduced ejection fraction
K_a	absorption rate constant
KCl	potassium chloride
KNO_3	potassium nitrate
C_{max}	maximum plasma concentration

N	Newton
NO_3^-	nitrate
NO	nitric oxide
NO_2^-	nitrite
$\mathbf{t_{max}}$	time to maximum plasma concentration
V	volume of distribution
W	Watts

8. References

1. Reid KF, Fielding RA. Skeletal muscle power: a critical determinant of physical functioning in older adults. Exerc Sport Sci Rev. 2012;40(1):4–12. [PubMed: 22016147]
2. Sunnerhagen KS, Cider A, Schaufelberger M, Hedberg M, Grimby G. Muscular performance in heart failure. J Card Fail. 1998;4(2):97–104. [PubMed: 9730102]
3. Toth MJ, Shaw AO, Miller MS, VanBuren P, LeWinter MM, Maughan DW, et al. Reduced knee extensor function in heart failure is not explained by inactivity. Int J Cardiol. 2010;143(3):276–82. [PubMed: 19327849]
4. Okita K, Kinugawa S, Tsutsui H. Exercise intolerance in chronic heart failure--skeletal muscle dysfunction and potential therapies. Circ J. 2013;77(2):293–300. [PubMed: 23337207]
5. Roberts AW OS, Blakeslee L, Rabe MA. The Population 65 Years and Older in the United States: 2016. US Census Bureau, American Community Survey Reports, ACS-38 2018.
6. Hunter GR, Plaisance EP, Carter SJ, Fisher G. Why intensity is not a bad word: Optimizing health status at any age. Clin Nutr. 2018;37(1):56–60. [PubMed: 28214041]
7. Marechal G, Gailly P. Effects of nitric oxide on the contraction of skeletal muscle. Cell Mol Life Sci. 1999;55(8–9):1088–102. [PubMed: 10442090]
8. Stamler JS, Meissner G. Physiology of nitric oxide in skeletal muscle. Physiol Rev. 2001;81(1):209–37. [PubMed: 11152758]
9. Kaminski HJ, Andrade FH. Nitric oxide: biologic effects on muscle and role in muscle diseases. Neuromuscul Disord. 2001;11(6–7):517–24. [PubMed: 11525879]
10. Reid MB. Nitric oxide, reactive oxygen species, and skeletal muscle contraction. Med Sci Sports Exerc. 2001;33(3):371–6. [PubMed: 11252061]
11. Evangelista AM, Rao VS, Filo AR, Marozkina NV, Doctor A, Jones DR, et al. Direct regulation of striated muscle myosins by nitric oxide and endogenous nitrosothiols. PLoS One. 2010;5(6):e11209. [PubMed: 20585450]
12. Lamb GD, Westerblad H. Acute effects of reactive oxygen and nitrogen species on the contractile function of skeletal muscle. J Physiol. 2011;589(Pt 9):2119–27. [PubMed: 21041533]
13. Suhr F, Gehlert S, Grau M, Bloch W. Skeletal muscle function during exercise-fine-tuning of diverse subsystems by nitric oxide. Int J Mol Sci. 2013;14(4):7109–39. [PubMed: 23538841]
14. Di Massimo C, Lo Presti R, Corbacelli C, Pompei A, Scarpelli P, De Amicis D, et al. Impairment of plasma nitric oxide availability in senescent healthy individuals: apparent involvement of extracellular superoxide dismutase activity. Clin Hemorheol Microcirc. 2006;35(1–2):231–7. [PubMed: 16899934]
15. Di Massimo C, Scarpelli P, Di Lorenzo N, Caimi G, di Orio F, Ciancarelli MG. Impaired plasma nitric oxide availability and extracellular superoxide dismutase activity in healthy humans with advancing age. Life Sci. 2006;78(11):1163–7. [PubMed: 16214176]

16. Nyberg M, Blackwell JR, Damsgaard R, Jones AM, Hellsten Y, Mortensen SP. Lifelong physical activity prevents an age-related reduction in arterial and skeletal muscle nitric oxide bioavailability in humans. J Physiol. 2012;590(21):5361–70. [PubMed: 22890714]
17. Richmonds CR, Boonyapisit K, Kusner LL, Kaminski HJ. Nitric oxide synthase in aging rat skeletal muscle. Mech Ageing Dev. 1999;109(3):177–89. [PubMed: 10576333]
18. Song W, Kwak HB, Kim JH, Lawler JM. Exercise training modulates the nitric oxide synthase profile in skeletal muscle from old rats. J Gerontol A Biol Sci Med Sci. 2009;64(5):540–9. [PubMed: 19304939]
19. Proctor DN, Parker BA. Vasodilation and vascular control in contracting muscle of the aging human. Microcirculation. 2006;13(4):315–27. [PubMed: 16611597]
20. Schrage WG, Eisenach JH, Joyner MJ. Ageing reduces nitric-oxide- and prostaglandin-mediated vasodilatation in exercising humans. J Physiol. 2007;579(Pt 1):227–36. [PubMed: 17138603]
21. Behnke BJ, Delp MD. Aging blunts the dynamics of vasodilation in isolated skeletal muscle resistance vessels. J Appl Physiol (1985). 2010;108(1):14–20. [PubMed: 19797684]
22. Hirai DM, Copp SW, Holdsworth CT, Ferguson SK, Musch TI, Poole DC. Effects of neuronal nitric oxide synthase inhibition on microvascular and contractile function in skeletal muscle of aged rats. Am J Physiol Heart Circ Physiol. 2012;303(8):H1076–84. [PubMed: 22923618]
23. Heffernan KS, Chale A, Hau C, Cloutier GJ, Phillips EM, Warner P, et al. Systemic vascular function is associated with muscular power in older adults. J Aging Res. 2012;2012:386387. [PubMed: 22966457]
24. Lundberg JO, Weitzberg E, Gladwin MT. The nitrate-nitrite-nitric oxide pathway in physiology and therapeutics. Nat Rev Drug Discov. 2008;7(2):156–67. [PubMed: 18167491]
25. Lundberg JO, Weitzberg E. NO generation from inorganic nitrate and nitrite: Role in physiology, nutrition and therapeutics. Arch Pharm Res. 2009;32(8):1119–26. [PubMed: 19727604]
26. Lundberg JO, Weitzberg E. NO-synthase independent NO generation in mammals. Biochem Biophys Res Commun. 2010;396(1):39–45. [PubMed: 20494108]
27. Piknova B, Park JW, Swanson KM, Dey S, Noguchi CT, Schechter AN. Skeletal muscle as an endogenous nitrate reservoir. Nitric Oxide. 2015;47:10–6. [PubMed: 25727730]
28. Piknova B, Park JW, Kwan Jeff Lam K, Schechter AN. Nitrate as a source of nitrite and nitric oxide during exercise hyperemia in rat skeletal muscle. Nitric Oxide. 2016;55–56:54–61. [PubMed: 27777094]
29. Gilliard CN, Lam JK, Cassel KS, Park JW, Schechter AN, Piknova B. Effect of dietary nitrate levels on nitrate fluxes in rat skeletal muscle and liver. Nitric Oxide. 2018;75:1–7. [PubMed: 29378248]
30. Park JW, Piknova B, Dey S, Noguchi CT, Schechter AN. Compensatory mechanisms in myoglobin deficient mice preserve NO homeostasis. Nitric Oxide. 2019;90:10–4. [PubMed: 31173908]
31. Wylie LJ, Park JW, Vanhatalo A, Kadach S, Black MI, Stoyanov Z, et al. Human skeletal muscle nitrate store: influence of dietary nitrate supplementation and exercise. J Physiol. 2019;597(23):5565–76. [PubMed: 31350908]
32. Srihirun S, Park JW, Teng R, Sawaengdee W, Piknova B, Schechter AN. Nitrate uptake and metabolism in human skeletal muscle cell cultures. Nitric Oxide. 2020;94:1–8. [PubMed: 31604144]
33. Kapil V, Webb AJ, Ahluwalia A. Inorganic nitrate and the cardiovascular system. Heart. 2010;96(21):1703–9. [PubMed: 20736204]
34. Siervo M, Lara J, Ogbonmwan I, Mathers JC. Inorganic nitrate and beetroot juice supplementation reduces blood pressure in adults: a systematic review and meta-analysis. J Nutr. 2013;143(6):818–26. [PubMed: 23596162]
35. Jones AM. Dietary nitrate supplementation and exercise performance. Sports Med. 2014;44 Suppl 1:S35–45. [PubMed: 24791915]
36. McMahon NF, Leveritt MD, Pavey TG. The Effect of Dietary Nitrate Supplementation on Endurance Exercise Performance in Healthy Adults: A Systematic Review and Meta-Analysis. Sports Med. 2017;47(4):735–56. [PubMed: 27600147]
37. Ashworth A, Bescos R. Dietary nitrate and blood pressure: evolution of a new nutrient? Nutr Res Rev. 2017;30(2):208–19. [PubMed: 28511731]

38. James PE, Willis GR, Allen JD, Winyard PG, Jones AM. Nitrate pharmacokinetics: Taking note of the difference. Nitric Oxide. 2015;48:44–50. [PubMed: 25937621]
39. van Velzen AG, Sips AJ, Schothorst RC, Lambers AC, Meulenbelt J. The oral bioavailability of nitrate from nitrate-rich vegetables in humans. Toxicol Lett. 2008;181(3):177–81. [PubMed: 18723086]
40. Hunault CC, van Velzen AG, Sips AJ, Schothorst RC, Meulenbelt J. Bioavailability of sodium nitrite from an aqueous solution in healthy adults. Toxicol Lett. 2009;190(1):48–53. [PubMed: 19576277]
41. Greenway FL, Predmore BL, Flanagan DR, Giordano T, Qiu Y, Brandon A, et al. Single-dose pharmacokinetics of different oral sodium nitrite formulations in diabetes patients. Diabetes Technol Ther. 2012;14(7):552–60. [PubMed: 22468627]
42. Wagner DA, Schultz DS, Deen WM, Young VR, Tannenbaum SR. Metabolic fate of an oral dose of 15N-labeled nitrate in humans: effect of diet supplementation with ascorbic acid. Cancer Res. 1983;43(4):1921–5. [PubMed: 6831427]
43. Jungersten L, Edlund A, Petersson AS, Wennmalm A. Plasma nitrate as an index of nitric oxide formation in man: analyses of kinetics and confounding factors. Clin Physiol. 1996;16(4):369–79. [PubMed: 8842573]
44. Webb AJ, Patel N, Loukogeorgakis S, Okorie M, Aboud Z, Misra S, et al. Acute blood pressure lowering, vasoprotective, and antiplatelet properties of dietary nitrate via bioconversion to nitrite. Hypertension. 2008;51(3):784–90. [PubMed: 18250365]
45. Kapil V, Milsom AB, Okorie M, Maleki-Toyserkani S, Akram F, Rehman F, et al. Inorganic nitrate supplementation lowers blood pressure in humans: role for nitrite-derived NO. Hypertension. 2010;56(2):274–81. [PubMed: 20585108]
46. Spiegelhalder B, Eisenbrand G, Preussmann R. Influence of dietary nitrate on nitrite content of human saliva: possible relevance to in vivo formation of N-nitroso compounds. Food Cosmet Toxicol. 1976;14(6):545–8. [PubMed: 1017769]
47. Duncan C, Dougall H, Johnston P, Green S, Brogan R, Leifert C, et al. Chemical generation of nitric oxide in the mouth from the enterosalivary circulation of dietary nitrate. Nat Med. 1995;1(6):546–51. [PubMed: 7585121]
48. Lundberg JO, Weitzberg E, Cole JA, Benjamin N. Nitrate, bacteria and human health. Nat Rev Microbiol. 2004;2(7):593–602. [PubMed: 15197394]
49. Carlstrom M, Montenegro MF. Therapeutic value of stimulating the nitrate-nitrite-nitric oxide pathway to attenuate oxidative stress and restore nitric oxide bioavailability in cardiorenal disease. J Intern Med. 2019;285(1):2–18. [PubMed: 30039620]
50. Carter SJ, Gruber AH, Raglin JS, Baranauskas MN, Coggan AR. Potential health effects of dietary nitrate supplementation in aging and chronic degenerative disease. Med Hypotheses. 2020;141:109732.
51. Webb DJ, Freestone S, Allen MJ, Muirhead GJ. Sildenafil citrate and blood-pressure-lowering drugs: results of drug interaction studies with an organic nitrate and a calcium antagonist. Am J Cardiol. 1999;83(5A):21C–8C. [PubMed: 10073779]
52. Montenegro MF, Sundqvist ML, Larsen FJ, Zhuge Z, Carlstrom M, Weitzberg E, et al. Blood Pressure-Lowering Effect of Orally Ingested Nitrite Is Abolished by a Proton Pump Inhibitor. Hypertension. 2017;69(1):23–31. [PubMed: 27802417]
53. Kass DA, Takimoto E, Nagayama T, Champion HC. Phosphodiesterase regulation of nitric oxide signaling. Cardiovasc Res. 2007;75(2):303–14. [PubMed: 17467673]
54. Coggan AR, Leibowitz JL, Kadkhodayan A, Thomas DP, Ramamurthy S, Spearie CA, et al. Effect of acute dietary nitrate intake on maximal knee extensor speed and power in healthy men and women. Nitric Oxide. 2015;48:16–21. [PubMed: 25199856]
55. Govoni M, Jansson EA, Weitzberg E, Lundberg JO. The increase in plasma nitrite after a dietary nitrate load is markedly attenuated by an antibacterial mouthwash. Nitric Oxide. 2008;19(4):333–7. [PubMed: 18793740]
56. Coggan AR, Hoffman RL, Gray DA, Moorthi RN, Thomas DP, Leibowitz JL, et al. A single dose of dietary nitrate increases maximal knee extensor angular velocity and power in healthy older men and women. J Gerontol A Biol Sci Med Sci. 2019.

57. Coggan AR, Broadstreet SR, Mikhalkova D, Bole I, Leibowitz JL, Kadkhodayan A, et al. Dietary nitrate-induced increases in human muscle power: high versus low responders. Physiol Rep. 2018;6(2).

58. Nyakayiru J, Kouw IWK, Cermak NM, Senden JM, van Loon LJC, Verdijk LB. Sodium nitrate ingestion increases skeletal muscle nitrate content in humans. J Appl Physiol (1985). 2017;123(3):637–44. [PubMed: 28663382]

59. Miller GD, Marsh AP, Dove RW, Beavers D, Presley T, Helms C, et al. Plasma nitrate and nitrite are increased by a high-nitrate supplement but not by high-nitrate foods in older adults. Nutr Res. 2012;32(3):160–8. [PubMed: 22464802]

60. Wilkerson DP, Hayward GM, Bailey SJ, Vanhatalo A, Blackwell JR, Jones AM. Influence of acute dietary nitrate supplementation on 50 mile time trial performance in well-trained cyclists. Eur J Appl Physiol. 2012;112(12):4127–34. [PubMed: 22526247]

61. McDonagh STJ, Wylie LJ, Webster JMA, Vanhatalo A, Jones AM. Influence of dietary nitrate food forms on nitrate metabolism and blood pressure in healthy normotensive adults. Nitric Oxide. 2018;72:66–74. [PubMed: 29223585]

62. Chirinos JA, Akers SR, Trieu L, Ischiropoulos H, Doulias PT, Tariq A, et al. Heart Failure, Left Ventricular Remodeling, and Circulating Nitric Oxide Metabolites. J Am Heart Assoc. 2016;5(10).

63. Kapil V, Khambata RS, Jones DA, Rathod K, Primus C, Massimo G, et al. The Noncanonical Pathway for In Vivo Nitric Oxide Generation: The Nitrate-Nitrite-Nitric Oxide Pathway. Pharmacol Rev. 2020;72(3):692–766.

64. Holford NH. A size standard for pharmacokinetics. Clin Pharmacokinet. 1996;30(5):329–32. [PubMed: 8743333]

65. Schultz DS, Deen WM, Karel SF, Wagner DA, Tannenbaum SR. Pharmacokinetics of nitrate in humans: role of gastrointestinal absorption and metabolism. Carcinogenesis. 1985;6(6):847–52. [PubMed: 3159503]

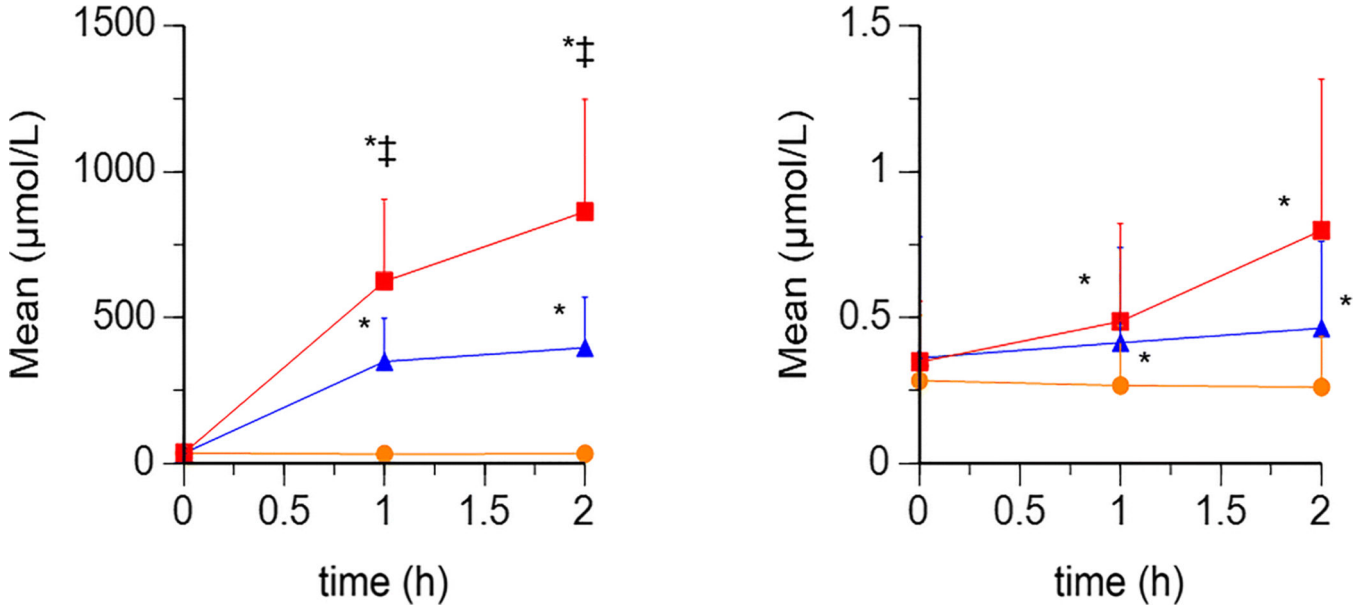

Fig. 1.

NO_3^- (left), NO_2^- (right) concentrations in plasma pre-dose, and at 1- and 2-hours following oral placebo or NO_3^- administration to a total of 42 patients, 37 of which were administered in a double-blinded randomized crossover fashion, and the remaining five given a single 10 mmol NO_3^- dose. Concentrations are presented as mean ± standard deviation following placebo (orange circles), an average NO_3^- dose of 11.6 mmol (blue triangles), or an average NO_3^- dose of 24.3 mmol (red squares). The number of samples for NO_3^- and NO_2^- at baseline was 154 and 153, respectively. The number of NO_3^- and NO_2^- samples was 41 and 14, respectively, at the 11.6 mmol and 24.3 mmol doses at each of the 1- and 2-hour times. *Significantly different from placebo ($p < 0.05$). ‡Significantly different from 11.6 mmol ($p < 0.05$)

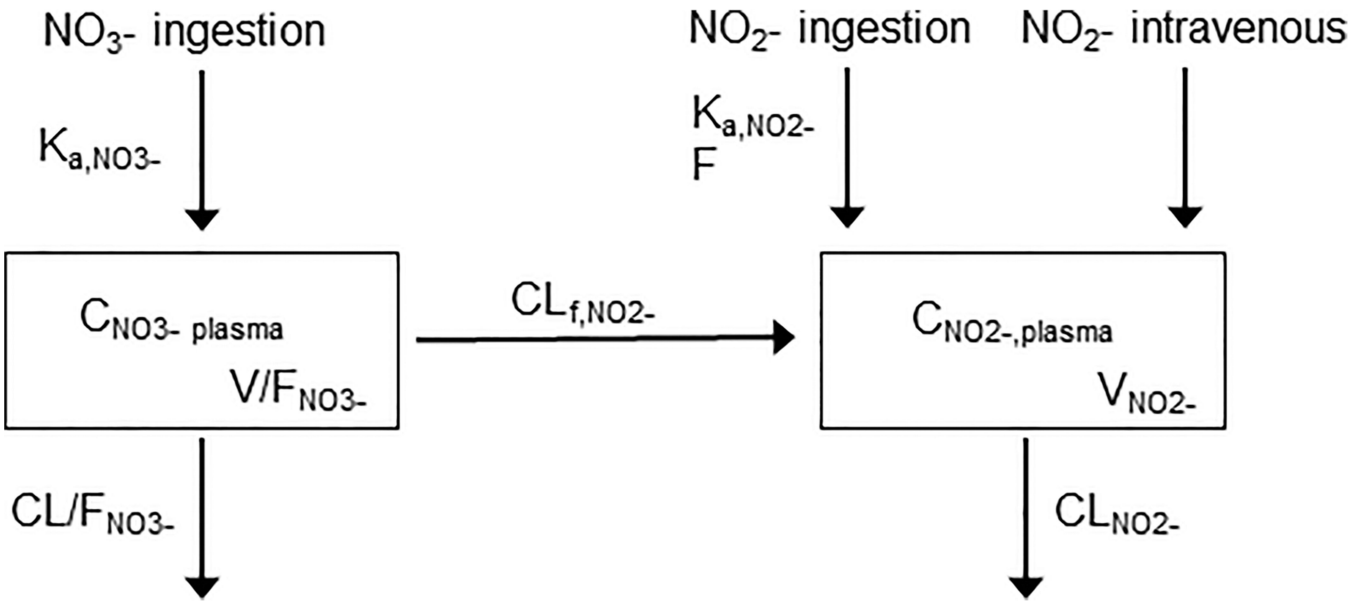

Fig. 2.

Structure of final model combining concentration changes over time in plasma NO_3^- and NO_2^- following oral NO_3^- ingestion. Abbreviations: C (concentration), V (volume of distribution), CL (elimination clearance), K_a (oral absorption rate constant), CL_f (formation clearance of NO_{2-})

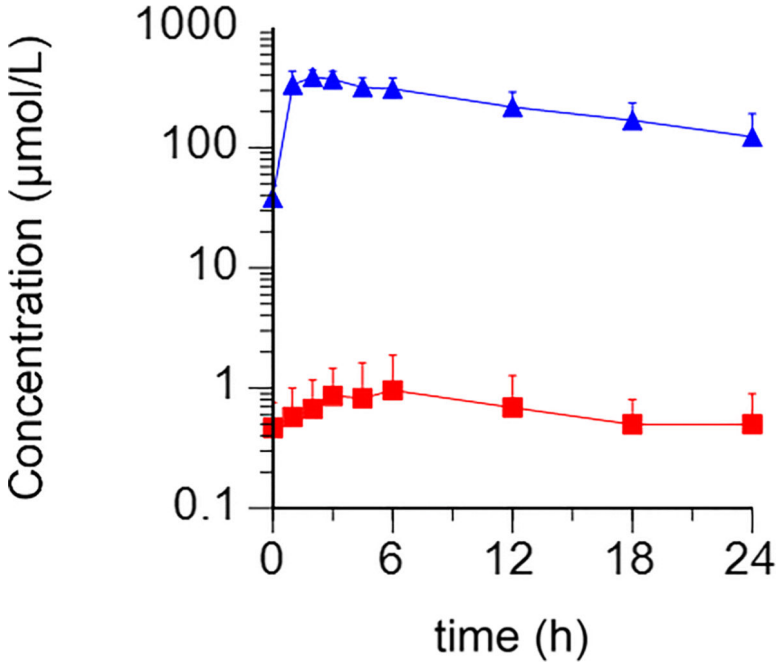

Fig. 3.

Average concentrations of plasma NO_3^- and NO_2^- observed in five patients with HFrEF following a 10 mmol dose of $KN0_3$ Results are presented as the mean ± standard deviation. NO_3^- concentrations are shown as blue triangles, and NO_2^- concentrations as red squares

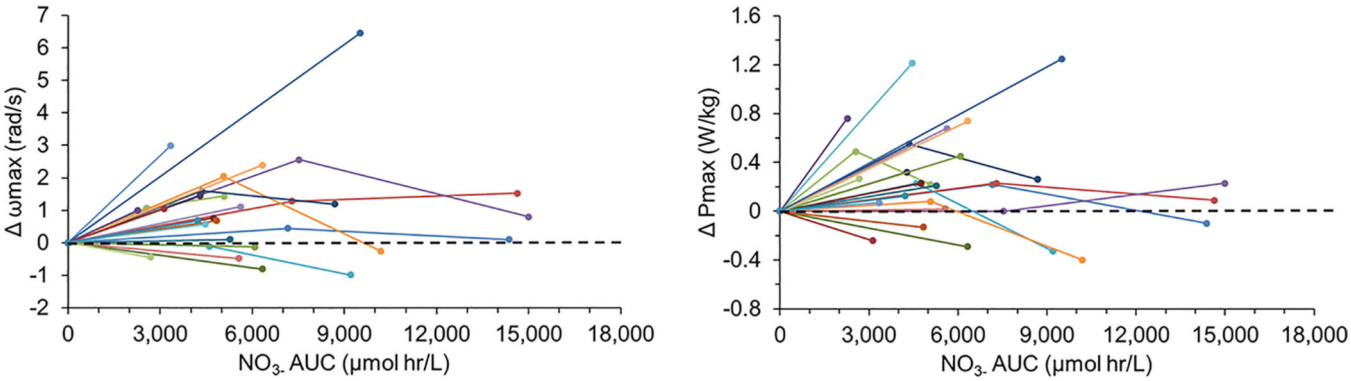

Fig. 4.

Relationship between NO_3^- $AUC_{0–24h}$ and change in maximal angular velocity (left) and power (right) of knee extension. Each line represents a subject. There were 23 subjects in which both NO_3^- exposure and muscle performance were measured

Table I.

Characteristics of subjects included in pharmacokinetic model development.

Characteristic	HFrEF (n = 28)	Elderly (n = 14)
Sex (Percent Male)	68	43
Race (White/Black/Asian)	23/4/1	12/2/none
Age (years) Mean	54.6	71.1
SD	12.12	4.50
Range	37 – 79	65 – 79
Body mass (Kg) Mean	99.0	73.8
SD	27.30	12.44
Range	43.2 – 173.9	55.4 – 98.0
Body mass index (Kg/m^2) Mean	32.5	25.4
SD	7.01	3.43
Range	19.1 – 45.7	21.1 – 30.6

HFrEF (Heart Failure reduced Ejection Fraction). Elderly defined as > 65 years.

Table II.

Pharmacokinetic parameter estimates of plasma NO_3^- and NO_2^- following oral ingestion of NO_3^-.

		Final model		Bootstrap Analysis	
Molecular Form	**Parameter**	**Estimate**	**RSD (%)**	**Median**	**5–95th percentile**
NO_{3-}	V/F (L)	20.0	4.3	20.0	17.9 – 22.2
	CL/F (L/h)	2.0	15.5	2.0	1.3 – 2.6
	K_a (h^{-1})	1.0	16.1	1.0	0.7 – 1.5
	baseline (μM)	31.1	7.5	31.0	26.4 – 36.0
	Covariate (BW on V)	0.92	17.1	0.93	0.64 – 1.35
	IIV (CV %)				
	Ka	74.0	32.9	74.8	72.7 – 76.9
	baseline	52.6	22.2	51.8	51.0 – 52.6
	RUV (%)	25.2	8.7	24.8	20.8 – 28.9
NO_{2-}	V (L)	84.5	8.6	80.3	51.2 – 105.5
	CL (L/h)	134.5	1.7	132.1	56.4 – 137.4
	CL_f (L/h)	0.05	25.8	0.04	0.03 – 0.07
	K_a (h^{-1})	6.4	47.0	8.6	4.1 – 24.5
	F (%)	1.0	1.4	1.0	0.5 – 1.0
	baseline (μM)	0.23	12.9	0.24	0.17 – 0.30
	IIV (CV %)				
	CL_f	130.5	39.2	128.2	123.3 – 133.1
	baseline	104.2	21.2	101.1	99.2 – 103.0
	RUV (%)	32.1	8.8	31.6	27.1 – 37.8

Abbreviations: V (volume of distribution), CL (elimination clearance), K_a (oral absorption rate constant), BW (body weight), CL_f (formation clearance of NO_2^-), F (bioavailability), baseline (endogenous concentration), IIV refers to inter-subject variability, expressed as coefficient of variation (CV, %) and calculated as $CV\ (\%) = \sqrt{\exp(\omega^2) - 1}\ x\ 100$. RUV is residual unexplained variability. RSD is relative standard deviation of the estimated parameter.